ORIGINAL RESEARCH

Cubosomes as Delivery System to Repositioning Nitrofurantoin in Breast Cancer Management

Dina Louis [iD][1,2],*, Christianne Mounir Zaki Rizkalla[1], Amira Rashad[3],*

[1]Department of Pharmaceutics and Industrial Pharmacy, Faculty of Pharmacy, Cairo University, Cairo, Egypt; [2]Department of Pharmaceutics, Faculty of Pharmacy and Drug Technology, Egyptian Chinese University, Cairo, Egypt; [3]Department of Pharmaceutical Technology, Faculty of Pharmacy, Heliopolis University, Cairo, Egypt

*These authors contributed equally to this work

Correspondence: Dina Louis, Department of Pharmaceutics and Industrial Pharmacy, Faculty of Pharmacy, Cairo University, Kasr Eleini Street, Cairo, 11562, Egypt, Tel +202 01228866769, Email dina.nassif@pharma.cu.edu.eg

Purpose: Nitrofurantoin (NITRO), a long-standing antibiotic to treat urinary tract infections, is activated by Nitro reductases. This activation mechanism has led to its exploration for repositioning applications in controlling and treating breast cancer, which express a Nitro reductase gene.

Methods: NITRO Cubosomes were developed using hot homogenization according to 2^3-full factorial design. The factors studied included the ratio of drug to oily phase (1:10 and 2:10), the ratio of oily to aqueous phase (1:10 and 1:5), and the ratio of Glyceryl mono-oleate (GMO) to Poloxamer 407 (PX407) (0.25:1 and 0.5:1). A total of 8 systems were proposed and evaluated by measuring particle size, zeta potential, polydispersity index, and percentage of entrapment efficiency.

Results: S6 (1:10 drug: oily phase, 1:5 oily: aqueous phase and 0.5:1 GMO: PX407) with particle size 45.5 ±c1.1 nm and an entrapment efficiency of 98.6 ± 1.8% exhibited highest desirability and was selected for further analysis. The morphology of S6 was examined using TEM microscopy. The activation of NITRO from S6 reflected on intracellular viability of MCF-7 breast cancer cell line was investigated by an MTT assay. The findings indicated that S6 had the lowest IC50 value (83.99 ± 0.15 μg g/mL) compared to Free NITRO (174.54 ± 1.36 μg g/mL), suggesting enhanced efficacy compared to free NITRO.

Conclusion: Nitrofurantoin cubosomes can be candidates for repositioning in breast cancer management after encouraging further stability and in-vivo studies.

Keywords: nitro reductase, glyceryl monooleate, Poloxamer 407, MTT assay, factorial design

Introduction

Cancer, a complex and multifactorial disease, includes the abnormal, uncontrollable cell growth and a continuous change in cell genome, resulting in the appearance of cancerous features within normal cells.[1,2] The main approach of any cancer therapy is to limit tumour growth, metastases, and prevent retrogression after elimination, resulting in prolongation of the life of the patient.[3] There are problems associated with common methods used in cancer therapy such as surgery, chemotherapy, and radiation. These problems include resistance to treatment, major side effects and absence of specific site delivery.[4] Hence, these methods are usually insufficient to produce results satisfactory to the patients. That necessitated the conduction of new studies to discover novel treatments.[5]

It was reported by the World Health Organization that about 2.3 million women suffered from breast cancer in 2020 and 0.5 million deaths annually.[6,7] A widely used treatment is radiotherapy,[8] in addition to several conventional chemotherapies.[9] The use of nano-carriers has been introduced in cancer therapy.[10] These involved the application of liposomes, polymeric nanoparticles, polymeric micelles, dendrimers,[11] magnetic nanoparticles,[12] and pH-sensitive nano-vehicles.[13] Photodynamic therapy has also been introduced as an effective treatment for cancer.[14] It involves the use of laser light, which is a specific and readily acceptable treatment by the patient. Photodynamic therapy also introduced the use of femto-laser in cancer treatment.[15]

6173

'Drug repositioning' describes the use of a drug in an indication apart from that to which it was originally approved. It has raised interest as it represents an alternative to new drug synthesis. An advantage of repositioning is the data available to researches. It also waives or reduces the studies that are required to investigate drug pharmacokinetics and toxicity.[16]

Nitrofurantoin (NITRO) is a nitrofuran derivative (1-[(E)-(5-nitrofuran-2-yl) methyl ideneamino] imidazolidine-2,4-dione) synthesized from hydantoin that is used to prevent and treat infections of the urinary tract. The mechanism of action of the drug involves inhibition of the synthesis of bacterial DNA. The nitro-group of the drug is reduced by the bacterial flavour-enzymes (Nitro reductase enzymes),[17] leading to the formation of reactive intermediates and consequent formation of hydroxyl radicals. These radicals can interact with DNA causing inhibition of nucleic acid synthesis, and brings about breaks in single- or double-strand DNA.[18,19]

However, recent studies have shown that nitrofurantoin may also have cytotoxic effects on tumour cells that express Nitro reductase.[5] In vitro studies have demonstrated that nitrofurantoin could inhibit the growth of various cell line-cancers, including colon, prostate, and breast cancer cells.[20]

Accordingly, nitro compounds having an antimicrobial action exhibiting an enzymatic bio-reduction of the nitro group result in products interacting with the biomolecules that are essential for the viability of cells. Consequently, these compounds possess anticancer activity against solid tumours containing hypoxic areas.[21] The selective cytotoxic effect of nitrofurantoin within hypoxic solid tumour cells[22] is a result of its reduction to a biologically active form in a hypoxic medium.

Nitrofurantoin belongs to class IV of the Biopharmaceutics Classification System. It exhibits both poor solubility and permeability.[23] Hence, improved bioavailability can be ensured by using a carrier system that enhances poor-water solubility as well as improves permeability.

Nanotechnology has significantly influenced cancer treatment by improving drug delivery system efficiency. Nanoparticles (NPs) offer benefits such as better pharmacokinetics, precise targeting of tumor cells, reduced side effects, and overcoming drug resistance.[24] These NPs are designed based on tumor characteristics and work by targeting tumor cells, releasing drugs to induce cell death. They also help deliver poorly soluble drugs into circulation, increase drug half-life, and protect normal cells from toxicity, thereby reducing the adverse effects of cancer therapy.[25] For example, nanomaterials such as gold, silver, and copper possess remarkable properties, making them highly effective in creating immunosensors. Their application in diagnostics of cancer has yielded outstanding results.[26]

Lipid-based nanoparticles play a major role in improving both drug solubility and permeability.

Cubosomes are among the lipid-based nanoparticles.[27] These nanoparticles are Liquid Crystals (LCNs), which are widely accepted and utilized as drug delivery systems in diseases like cancer.[28] The cubosomes have a marked advantage of being able to tune the membrane curvatures irrespective of nanoparticle diameter across large lengths. Accordingly, they promote drug targeting, extended half-life and sustained release.[28] Cubosomes are self-structured nanoparticles, derived from bulk bi-continuous cubic-phase lipids, stabilized by pluronics. Cubosomes can be prepared using amphi-philic lipids such as Glyceryl Mono-oleate (GMO) which self-assemble in a liquid state to form cubosomes.[29] Phytantriol can also replace GMO, especially in cosmetic products.[30] The bi-continuous phase organizes in a honeycomb three-dimensional structures. They possess cavern-like structure, which allow efficient drug loading.[31–33] Preparation of cubosomes involves top-down[34] or bottom-up methods.[35] Cubosomes allow a better loading of hydrophobic drugs compared to liposomes.[36] Evaluation and characterization of cubosomes can be done by electron microscopic imaging, X-ray scattering, particle size distribution, and entrapment efficiency determination.[37]

The cubosome's small size leads to an improvement in drug permeation and retention at the cancer site,[37] which makes them efficient for targeted delivery systems. This is the main requisite for cancer treatment. Moreover, Cubosomes are advantageous over the liposomes in that they can accommodate greater volumes, which help incorporation of larger quantities for drug. That resulted in improved drug loading, and a lower viscosity.[38,39] Also, cubosomes, can accommodate water-soluble drugs within their bilayers. These loaded cubosomes break by intestinal lipases into smaller bio adhesive particles with prolonged contact with intestinal walls, which promotes drug absorption and bioavailability.[40]

These Cubosomes are versatile carriers with a theranostic efficiency that is promising. They can be prepared to be administered orally, topically, or intravenously. Recent research has helped to improve the preparation, efficacy, evaluation, target selection, and control of drug release pattern of the loaded anticancer drugs.[28] Cubosomes were

successfully used to deliver 5-Fluorouracil, Cisplatin and paclitaxel, Cisplatin and paclitaxel, Temozolomide, Doxorubicin and, Icarin to various cancer cells.[41]

In this study, NITRO is intended to be repurposed in the control of breast cancer cells that express the nitro reductases, necessary for NITRO activation. It was to be formulated as Cubosomes to benefit from its unique properties in drug delivery to ensure the effectiveness of NITRO.

Materials and Methods

Materials

Nitrofurantoin (NITRO) (a kind gift from Sinochem Jiangsu, China). Poloxamer 407 (PX407) (Fisher Scientific, UK), Glyceryl mono oleate (GMO) 90–95% and dimethyl formamide (DMF) (Sigma Aldrich, USA). All the other chemicals were of analytical reagent grade.

Methods

Preparation of NITRO- Cubosomes (NITRO-Cs) Systems

The cubosome Oily (lipid) phase components, namely, Poloxamer (PX 407) and Glyceryl mono oleate (GMO), were weighed according to the specific weight ratios. They were melted using a hot water bath at 60 °C until the formation of a uniform dispersion. The molten oily dispersion was stirred well before adding the corresponding accurately weighed amount of NITRO. Then, the oily dispersion was exposed to a 10-minute high speed homogenization (High-speed homogenizer, Heidolph Diax 900, Germany) at 10000rpm during which distilled water (preheated to 60 °C) was added drop-wise. That was followed by exposure for two minutes to ultrasonic sound waves (Probe Sonicator, GE 130, China) which were operated as pulses every 2 seconds to ensure breaking up agglomerates that could exist in the dispersion. Then, the systems were allowed to cool and stored for 48 hours in amber-coloured glass vials before further investigation.[42]

Full Factorial Design

The design of the experiment was built on a 2^3-full factorial design using the software Design-Expert VR (V.7.0.0, Stat-Ease Inc., Minneapolis, USA). The study aimed to identify the effect of three independent variables on specific responses. The factors (independent variables) under investigation were the drug: oily phase (X1), oily: aqueous phase (X2), and GMO: PX 407 (X3) ratios. The responses were Particle Size (PS) of produced cubosomes (R1), Zeta potential (ZP) value (R2), Polydispersity Index (PDI) (R3), and Percentage entrapment efficiency (%EE) (R4). Optimization was set to achieve the minimum PS and PDI and maximum ZP and %EE to obtain the system with the highest desirability. Table 1 summed up the factors, their levels, and the constraints involved in the preparation and optimization of NITRO-Cs.

Table 1 2^3-Factorial design independent variables, their levels, responses and constraints for NITRO-Cs systems.

Table 1 2^3-Factorial Design Independent Variables, Their Levels, Responses and Constraints for NITRO-Cs Systems

Factors (Independent Variables)	Levels	
	Minimum	**Maximum**
Drug: Oily phase ratio (X1)	1:10	2:10
Oily: Aqueous phase ratio (X2)	1:10	1:5
GMO: PX 407 ratio (X3)	0.25:1	0.5: 1
Responses	**Constraints**	
R1: Particle Size (PS)	Minimize	
R2: Zeta Potential (ZP)	Maximize	
R3: Polydispersity Index (PDI)	Minimize	
R4: Percentage entrapment efficiency (%EE)	Maximize	

Evaluation of NITRO- Cubosomes (NITRO-Cs)

Entrapment Efficiency Percentage (%EE)

The %EE was determined by the reported indirect method.[43] NITRO-Cs systems were exposed to centrifugation to separate the un-entrapped drug in the external phase (Cooling Centrifuge, Centurion Scientific K3 Series, Germany).[44] Samples of 2 mL were placed in Eppendorf tubes and exposed to centrifugation at 14000 rpm at 4°C for ten minutes. The high speed and cooling resulted in congealing and precipitation of the cubosomes, leaving behind the aqueous phase which contained the free un-entrapped drug. One millilitre of the supernatant was appropriately diluted to 25 mL with distilled water, and the UV absorbance of the samples was determined at λ max of 375 nm (UV spectrophotometer (Lab India UV-320, Mumbai, India).[45] The corresponding concentration of the free NITRO in the supernatant was then calculated based on a previously constructed calibration curve of Nitrofurantoin in distilled water. The measurements were repeated six times for each system. The entrapped amount of NITRO was calculated using the following equation:

$$\%EE = \frac{C\,total - C\,free}{C\,total} X100$$

Where C_{free} is the calculated amount of free NITRO and C_{total} is the total amount of NITRO present in one mL of cubosomes dispersion.

Particle Size (PS), Zeta Potential (ZP) and Polydispersity Index (PDI)

The mean PS and PDI of cubosomes as well as the ZP for the NITRO-Cs systems were measured utilizing the technique of laser diffraction through a Zeta sizer (Malvern, Nano Series ZS90, Malvern Instruments, Ltd., Worcestershire, UK). A sample (0.5 mL) was diluted appropriately using 30 mL of distilled water to get the required intensity of scattering. All measurements run at 25°C.[46,47]

In-Vitro Release Study

The profile of release of the highest desirability system with was studied. The dialysis membrane (Dialysis Tubing Cellulose Membrane, molecular weight cut-off 12,000–14,000, SERVA GmbH, Heidelberg, Germany) was employed in that study to evaluate the selected cubosomes formulation and the free drug.[48] One mL of the selected system (17 mg. mL) or an equivalent mass of free drug in 1mL saline phosphate buffer (PBS), pH 7.4, was placed inside a tube open from one side and sealed by the dialysis membrane on the other side. The tube was immersed in 50 mL PBS (pH 7.4) at 37±0.5°C and stirred at 150 rpm. Three-millilitre samples were withdrawn at time intervals of 0.5, 1, 2, 3, 4, 5, 6, and 12 hours and were compensated for by an equal amount of fresh buffered solution. The withdrawn samples were appropriately diluted with the buffered solution, and the drug was spectrophotometrically determined at λ max 375 nm. The experiment was run six times (per point). The percentage of released drug was calculated based on the ratio of the amount of released drug relative to the initial amount of drug within the dialysis bag. Release results for free NITRO and the optimized formulation were compared after 4 and 8 hours. Statistical analysis of the results was done using a Student's *T*-test.

Transmission Electron Microscope (TEM)

The images of the optimal NITRO-Cs system were captured for determining its shape using TEM (JEOL, JEM-1400 Electron Microscope, Japan). One drop of the optimized NITRO-Cs system was diluted with deionized water and placed on a copper grid that is coated with carbon, followed by 1% sodium phosphor-tungstate solution staining. The sample was left for air-drying at room temperature. Then, followed the examination at 200 kV power.[49]

Studies of Cell Survival Using MCF-7 Cells

The cytotoxic effect of NITRO-Cs optimal system was determined using MCF-7 breast cancer cells (Human Breast Cancer Cell-Line, VACSERA, Egypt sub-cultured from ATCC ® HTB-22™). An assay of MTT reduction was employed.[50] Inoculation of a tissue culture plate with 96-wells (Microtiter™) with 1×10^5 cells/mL was done, and it was incubated at 37°C for 24 hours to allow cell development and to make a complete cell monolayer. The plates contained the growth medium required for cell development (RPMI-1640 medium enriched with 1% l-glutamine, 10% inactivated foetal bovine serum, 50 µg/mL gentamycin, and HEPES buffer). The NITRO-Cs selected system was

compared to the free drug and the plain cubosomes (None-loaded Cubosomes). The samples under test were serially diluted (31.25–62.5- 125- 250- 500-1000 μg/mL) with the maintenance medium (RPMI medium with 2% serum) and an amount of 0.1mL of each serial dilution for each sample was inoculated into the wells (five replicas per dilution). These dilutions were compared to a control test (2 replicas). The plate was then incubated at 37°C before being examined. Cells were observed for any physical signs of toxicity, eg rounding, partial or complete loss of the monolayer, granulation, or cell shrinkage. Twenty microliters of MTT solution of concentration of 5mg/mL PBS (BIO BASIC CANADA INC) were added to each well and mixed by placing it on a shaker, at 150 rpm for 5 minutes. The plates were incubated (at 37°C, 5% CO_2) for 4 hours to allow the metabolism of MTT. Formazan (MTT metabolic product) was re-suspended in DMSO (200 ul) and mixed thoroughly. Reading optical density was done at 560 nm and the background was subtracted at 620 nm employing Biotek ELX800 micro-plate reader. Optical density was correlated directly to the quantity of cells.

Statistical Analysis

Design-Expert VR software (V.7.0.0, Stat-Ease Inc., Minneapolis, USA) and Microsoft Excel 2019 were used to run the full factorial design. ANOVA factorial compared the means at $p < 0.05$ level of significance with a Tukey post hoc test. Numerical optimization[51] was done according to the constraints indicated in Table 2. All experiments were repeated six times, and the results were displayed as mean± SD.

Results

All prepared NITRO-C systems were uniform milky yellow dispersions that did not show any aggregations. According to the experimental design, eight NITRO-loaded systems were examined whose composition and evaluation results are shown in Table 2.

Table 2 Composition and results of characterization of NITRO-Cs systems.

There was a significant effect of all variables, drug: oily phase ratio, oily: aqueous phase ratio, and GMO: PX407 ratio on PS ($p = 0.0006$). Low drug: oily phase ratio, high oily: aqueous phase ratio, and high GMO: PX407 ratios favoured low PS.

ZP was significantly affected by studied variables ($p = 0.0141$). An increase in ZP followed the increase in drug: oily phase ratio, increase in oily: aqueous phase ratio, and the increase in GMO: PX407 ratio.

The size distribution of the dispersion (PDI) was significantly affected by the studied variables ($p‹ 0.0001$). Low PDI was associated with a low drug: oily phase ratio, high oily: aqueous phase ratio, and high GMO: PX407 ratio.

Figure 1 illustrates the interaction between the studied variables and their effects on PS, ZP and PDI.

The desirability approach based on factorial design data analysis was used to achieve the numerical optimization. The analysis was done to determine the values for X1, X2 and X3 that will minimize system PS and PDI; and

Table 2 Composition and Results of Characterization of NITRO-Cs Systems

| S	Drug: Oily phase ratio (X1)	Oily: Aqueous phase ratio (X2)	GMO: PX407 ratio (X3)	PS (nm) (R1)	ZP (mV) (R2)	PDI (R3)	%EE (R4)
1	2:10	1:10	0.25:1	89.9±1.7	−19.4± 2.8	0.6± 0.0	98.7±1.9
2	1:10	1:5	0.25:1	34.5±0.1	−15.9±0.1	0.3± 0.0	98.6± 1.8
3	1:10	1:10	0.25:1	50.5±1.6	−16.1±0.4	0.5± 0.1	97.4±1.0
4	1:10	1:10	0.5:1	72.9±0.1	−7.9±2.2	0.4± 0.0	98.0±1.4
5	2:10	1:10	0.5:1	57.7±0.4	−8.2 ±0.8	0.4± 0.1	98.3±1.6
6	1:10	1:5	0.5:1	45.5±1.1	−13.4±0.6	0.3± 0.0	98.6±1.8
7	2:10	1:5	0.5:1	50.9±3.9	−23.8±1.4	0.4± 0.0	98.1±1.4
8	2:10	1:5	0.25:1	52.9±2.1	−8.6 ± 0.7	0.6± 0.1	97.9± 1.3

(A)

(B)

(C)
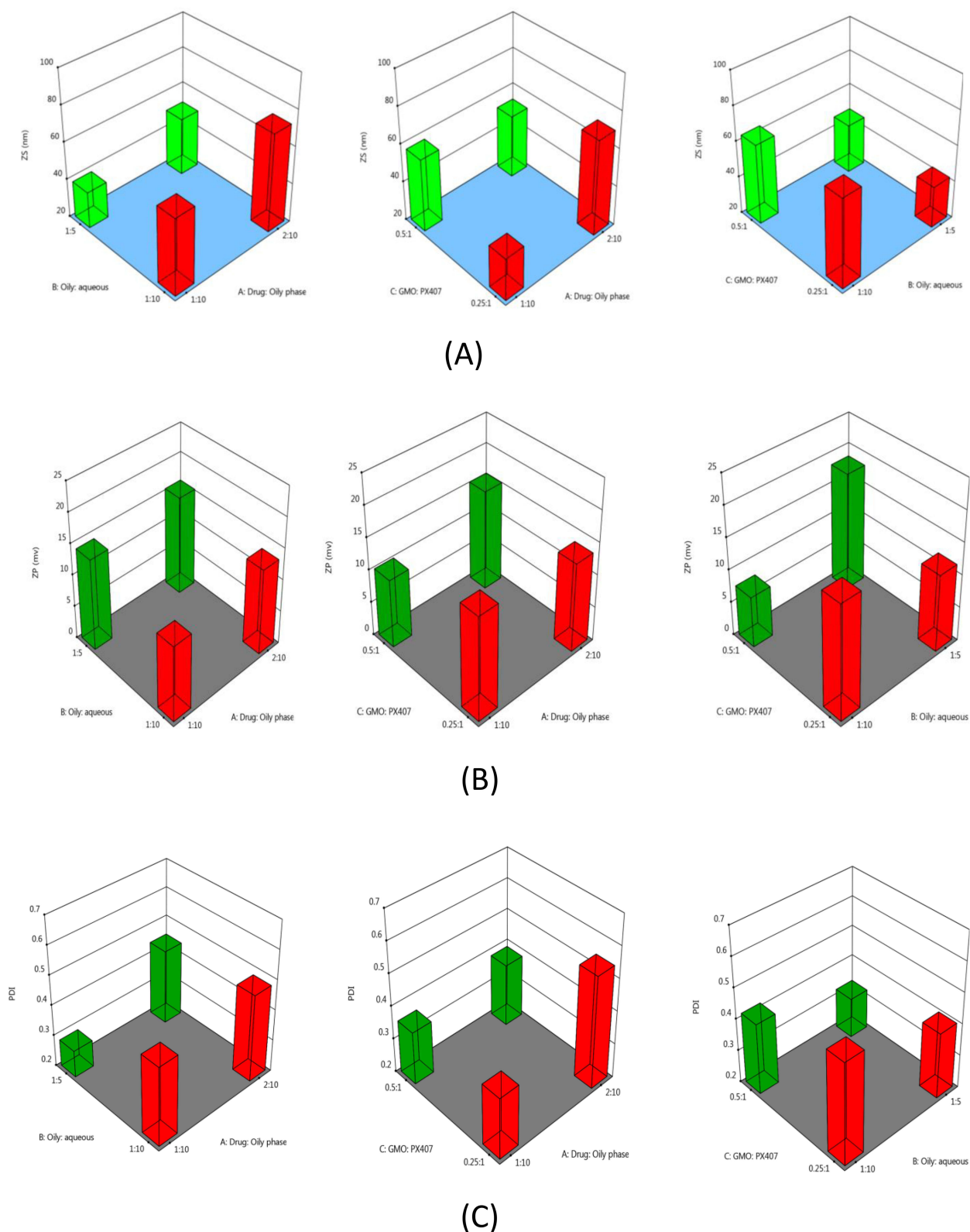
Figure I Effects of interactions between the studied factors on Nitrofurantoin cubosome system PS (**A**), ZP (**B**), and PDI (**C**).

maximize ZP and %EE. Desirability values ranged from 0 to 1. The optimized system was S6, which possessed the highest desirability (0.774). Its composition was 1:10 Drug: Oily phase ratio, 1:5 Oily: Aqueous phase ratio, and 0.5:1 GMO: PX407 ratio.
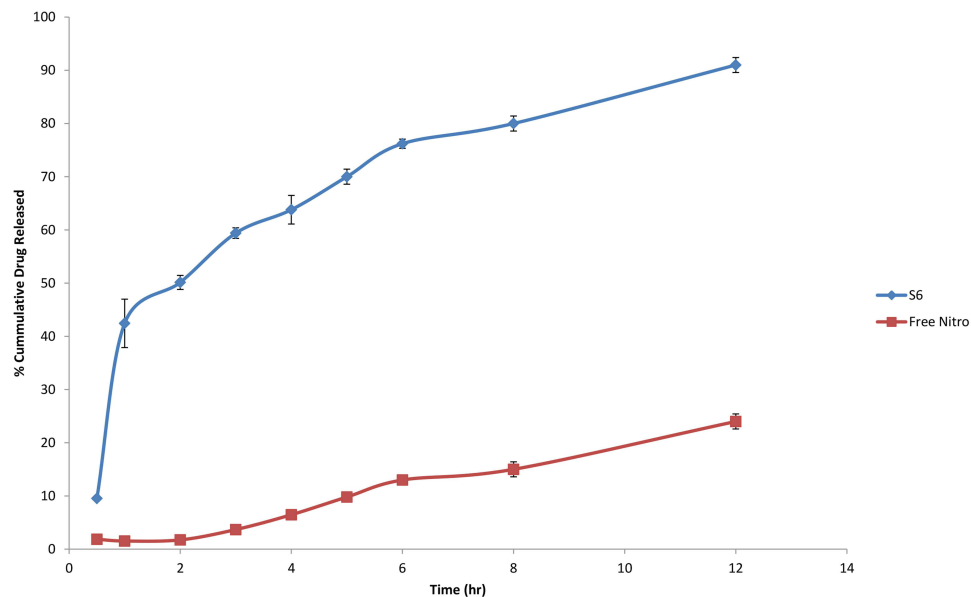
Figure 2 Cumulative Percentage of drug released from S6 Vs Free NITRO.

Accordingly, system S6 was considered for further investigation, where the release profile was studied. Figure 2 illustrates the release profile of NITRO from the S6 system against the free drug.

The figure shows the superiority of drug release from S6 compared to NITRO when compared after the passage of 4 hours ($p = 0.00055$) and 8 hours ($p = 0.000237$).

Kinetic analysis of the release of drug from S6 revealed zero-order release kinetics ($R^2 = 0.8929$ for zero order, $R^2 = 0.4689$ for first, $R^2 = 0.889$ for Higuchi model).

TEM photographs of S6 (Figure 3) showed spherical to polygonal structures of cubosomes. It was possible to identify a defined coat with dark colour and a core with a much lighter colour which consisted of the drug encapsulated. The particle size appeared to be below 50 nm.
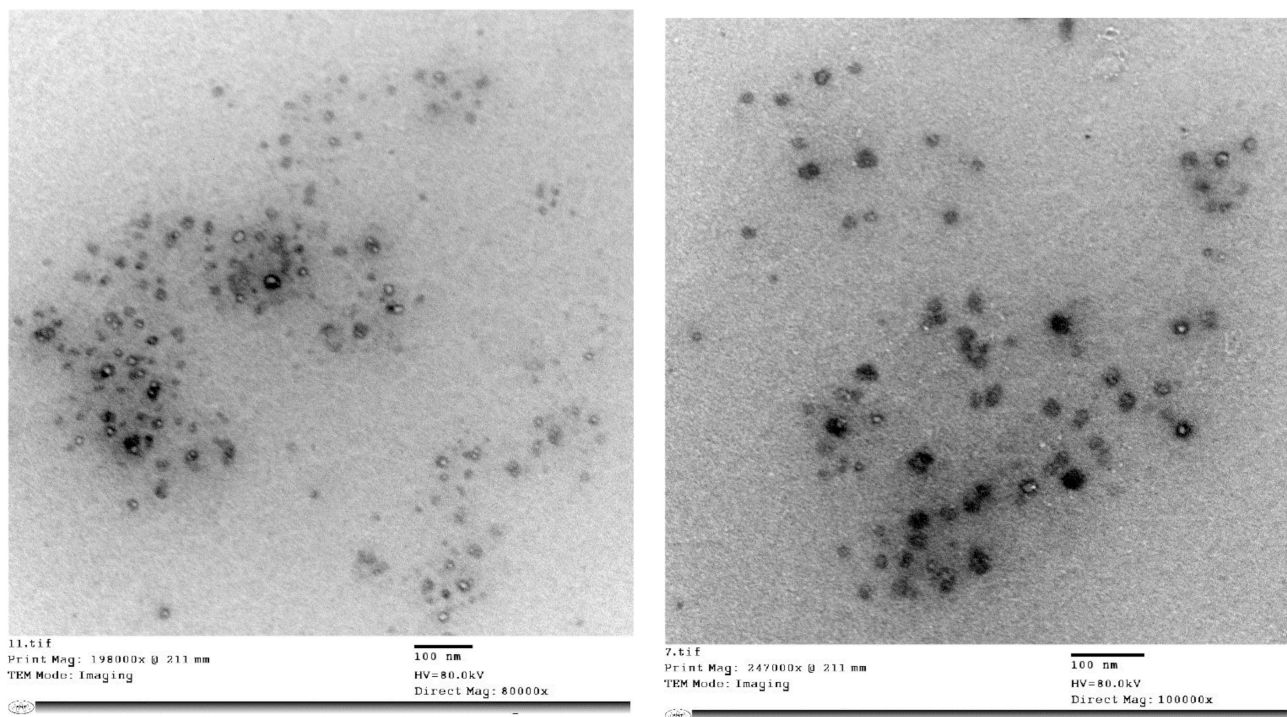

Figure 3 TEM photographs of S6.

S6 was tested for its cytotoxic effect on the MCF breast cancer cells. Serial dilutions of S6, free NITRO and none-loaded cubosomes were investigated for their cytotoxic effect. The following Figure 4 demonstrates the percentage cell viability of S6 compared to free NITRO, and the none-loaded cubosomes at such dilutions.

The figure revealed the superior cytotoxic effect of S6 compared to the free NITRO and None-loaded cubosomes. Calculations of IC50 revealed the effectiveness of S6 at lower concentrations as demonstrated in Figure 5.

ANOVA of the values of IC50 revealed a significantly lower value for S6 (83.99 ± 0.15 µg g/mL) compared to Free NITRO (174.54 ± 1.36 µg g/mL) and None-loaded Cubosomes (207.38 ± 0.59 µg g/mL) ($p = 0.000$).

The effect of S6, free NITRO, and None-loaded Cubosomes on the cell viability was reflected in cell morphology compared to the control cell group. Signs of cellular distress were observed in Figure 6 as evidenced by the presence of small rounded cells.
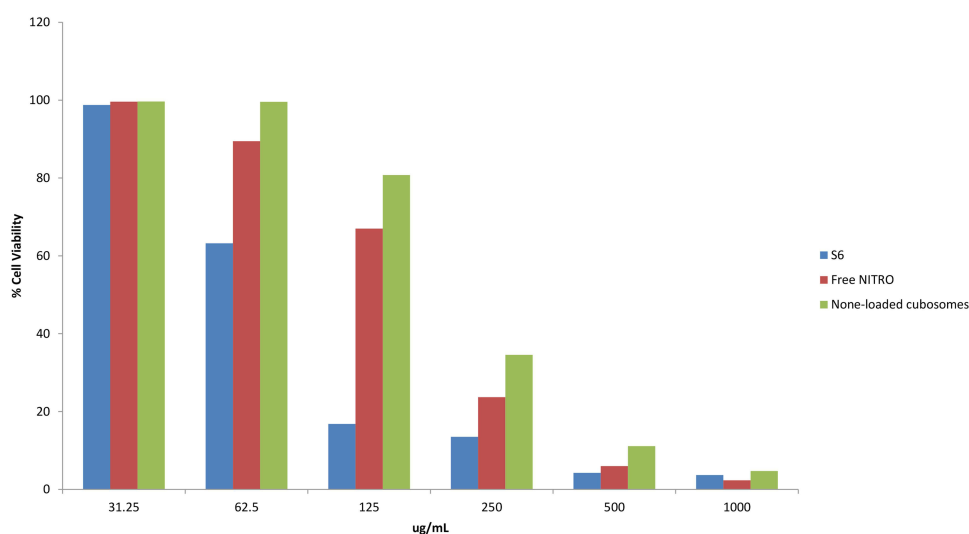

Figure 4 Effects of different dilutions of S6, Free NITRO and None-loaded Cubosomes on MCF-7 cells.
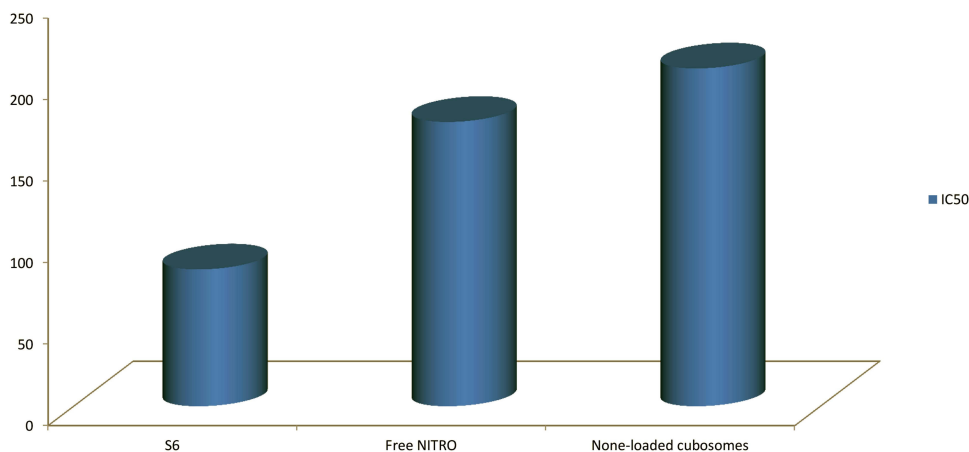

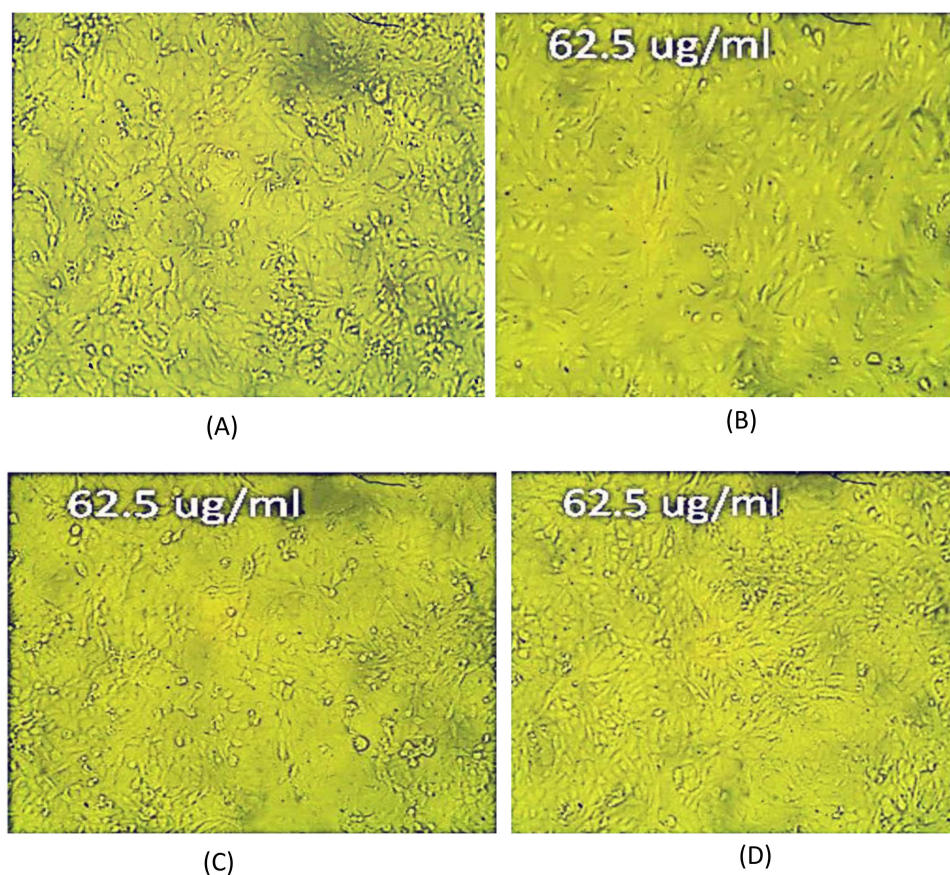**Figure 5** IC50 for S6 compared to free Nitro and None-loaded Cubosomes.

Figure 6 Inverted microscope photos of (**A**) Control MCF-7 cells; (**B**) 62.5 ug/mL of S6; (**C**) Free NITRO and (**D**) None-loaded Cubosomes.

Discussion

Based on reported results in Table 2, all NITRO-Cs systems showed high %EE, which ranged from 97.43% to 98.71%. ANOVA of the results revealed that high encapsulation efficiency was associated with a high oily: aqueous phase ratio and high GMO: PX407 ratio (p = 0.0007). That was due to the drug's poor water solubility. That rendered the drug embedded in the oily bilayer in the alkyl chains forming up GMO, irrespective of the amount of GMO present relative to the drug amount or water amount.[52,53]

An increase in PS was associated with increased drug ratio, which agreed with previous findings where increased particle size was associated with increased drug loading in Flurbiprofen preparation as cubosomes.[54] Although high percentages of PX407 (low GMO: PX407 ratio) favoured low PS, such high percentages could promote the formation of different vesicular structures along with cubosomes.[55] That accounted for reporting the relatively large size distribution (PDI) associated with a low GMO: PX407 ratio.

Prepared systems showed a negative value for ZP. That was attributed to the negatively charged free oleic acid molecules related to GMO structure.[56] A high ZP accompanied the high oily content imparted by a high GMO percentage (high GMO: PX407 ratio), which agreed with the literature in which cubosomes of Resveratrol with the highest GMO content exhibited the highest ZP.[57]

The optimized system as dictated by desirability calculation was found to be S6, and hence it was further investigated with respect to drug release, TEM and cytotoxicity assessment.

The release profile of free NITRO and S6 is demonstrated in Figure 2 which revealed the significant superiority of percentage of drug released from S6 compared to free NITRO after 4 hours (p = 0.00055) and after 8 hours (p = 0.000237). That was attributed to the ability of PX407 to solubilize NITRO and allowed its release from the cubosomes into the release medium.[58] The figure also revealed that S6 possessed two different rates of drug release: a first phase

with a higher rate of drug release, followed by a phase with slower rate. That could be attributed to the presence of the drug solubilized within the oily structure, which offered a large surface area (nano-size) for exposing the drug to the release medium. Later on, a slower release pattern was exhibited due to the diffusion of the drug from the tortuous structure of cubosomes into the release medium. Such results agreed with previous findings for the Clopidogrel Bisulphate cubosome release pattern that showed that biphasic pattern due to the large surface area associated with the nanoparticles.[27] The zero order release kinetics from S6 ensured constant rate for drug delivery over an extended period.[59]

Results of the studies done using MCF-7 cells demonstrated the ability of NITRO to penetrate the cell and induce distress and cytotoxicity whether in free form or cubosomal entrapment. The known mechanism of action for NITRO, as an old antibacterial, has been described based on its activation to highly electrophilic reactive intermediates, under the effect of Nitro reductases. Such intermediates attached ribosomal proteins, causing protein synthesis inhibition, resulting in a cell damaging action.[20] Studies revealed that the Nitro reductase enzyme is overexpressed by breast cancer cells.[60] Such finding implied that the presence of NITRO in the vicinity of breast cancer cells allowed its activation by the produced Nitro reductase. That resulted in the NITRO inhibitory effect on protein synthesis. Accordingly, NITRO was successful to induce a cytotoxic effect on MCF-7 cells whether as Free NITRO or as S6 (cubosomal system). The superiority of S6 over free NITRO, as evidenced by a significantly lower IC50 (83.99 ± 0.15 μg g/mL) compared to free NITRO (174.54 ± 1.36 μg g/mL), could be attributed to the encapsulation of NITRO into cubosomes. The small size of cubosomes as well as their ability to tune membrane curvatures helped improve drug retention as well as permeation through the cells.[28,31]

The observed cytotoxic effect of None-loaded Cubosomes was minimal as evidenced by a significantly higher IC 50 (207.38 ± 0.59 μg g/mL).[61] Such high concentrations, on the contrary, ensured the biocompatibility of None-loaded Cubosomes with normal cells when administered at the effective concentration of S6.

Conclusion

Accordingly, the long-known antibiotic NITRO, successfully used in urinary tract infection management, can regain attention by repositioning. NITRO, as a Class IV drug, can show enhanced solubility and improved cell penetration by encapsulation into cubosomes. NITRO Cubosomes were developed using hot homogenization according to 2^3-full factorial design. S6 (1:10 drug: oily phase, 1:5 oily: aqueous phase and 0.5:1 GMO: PX407) exhibited highest desirability and was selected for further analysis. In a cubosomal system (S6), NITRO could exhibit cytotoxic effects against breast cancer cells due to its activation by the Nitro reductase enzyme released by cancer cells and due to enhanced penetration facilitated by the cubosomal coat while maintaining the safety of the normal cells. Thus, NITRO, on regaining popularity in a new field of breast cancer management, can fulfil one of the aims of sustainable development. Hence, it is recommended to carry out further in-vivo and stability studies.

Disclosure

The author(s) report no conflicts of interest in this work.

References

1. Mansoori B, Mohammadi A, Davudian S, Shirjang S, Baradaran B. The different mechanisms of cancer drug resistance: a brief review. *Adv Pharm Bull*. 2017;7(3):339–348. doi:10.15171/apb.2017.041
2. Anand U, Dey A, Chandel AKS, et al. Cancer chemotherapy and beyond: current status, drug candidates, associated risks and progress in targeted therapeutics. *GENES DIS*. 2023;10(4):1367–1400. doi:10.1016/j.gendis.2022.02.007
3. Debela DT, Muzazu S, Heraro KD, et al. New approaches and procedures for cancer treatment: current perspectives. *SAGE Open Med*. 2021;9(1):1–10. doi:10.1177/20503121211034366
4. Chupradit S, Widjaja G, Radhi Majeed B, et al. Recent advances in cold atmospheric plasma (CAP) for breast cancer therapy. *Cell Biol Int*. 2023;47(2):327–340. doi:10.1002/cbin.11939
5. Moura C, Correia AS, Pereira M, Ribeiro E, Santos J, Vale N. Atorvastatin and nitrofurantoin repurposed in the context of breast cancer and neuroblastoma cells. *Biomedicines*. 2023;11(3):903–923. doi:10.3390/biomedicines11030903
6. Rabelo ACS, Guerreiro CA, Shinzato VI, Ong TP, Noratto G. Anthocyanins reduce cell invasion and migration through akt/mtor downregulation and apoptosis activation in triple-negative breast cancer cells: a systematic review and meta-analysis. *Cancers*. 2023;15(18):2300–2313. doi:10.3390/cancers15082300

7. El-Tanani M, Platt-Higgins A, Lee Y, et al. Matrix metalloproteinase 2 is a target of the RAN-GTP pathway and mediates migration, invasion and metastasis in human breast cancer. *Life Sci.* 2022;310(1):1–28. doi:10.1016/j.lfs.2022.121046

8. Guo Z, Zhang H, Fu Y, et al. Cancer-associated fibroblasts induce growth and radioresistance of breast cancer cells through paracrine IL-6. *Cell Death Discov.* 2023;9(6):1–10. doi:10.1038/s41420-023-01306-3

9. Hernandes EP, Lazarin-Bidóia D, Bini RD, Nakamura CV, Cótica LF, de Oliveira Silva Lautenschlager S. Doxorubicin-loaded iron oxide nanoparticles induce oxidative stress and cell cycle arrest in breast cancer cells. *Antioxidants.* 2023;12(2):273–289. doi:10.3390/antiox12020237

10. Ashrafizadeh M, Zarrabi A, Bigham A, et al. (Nano) platforms in breast cancer therapy: drug/gene delivery, advanced nanocarriers and immunotherapy. *Med Res Rev.* 2023;2(1):1–15.

11. Yang F, He Q, Dai X, Zhang X, Song D. The potential role of nanomedicine in the treatment of breast cancer to overcome the obstacles of current therapies. *Front Pharmacol.* 2023;14(1):1–12.

12. Dongsar TT, Dongsar TS, Abourehab MA, Gupta N, Kesharwani P. Emerging application of magnetic nanoparticles for breast cancer therapy. *Eur Polym J.* 2023;187(1):1–10. doi:10.1016/j.eurpolymj.2023.111898

13. Rajaei M, Rashedi H, Yazdian F, Navaei-Nigjeh M, Rahdar A, Díez-Pascual AM. Chitosan/agarose/graphene oxide nanohydrogel as drug delivery system of 5-fluorouracil in breast cancer therapy. *J Drug Deliv Sci Technol.* 2023;82(1):1–10.

14. Xu J, Lai Y, Wang F, et al. Dual stimuli-activatable versatile nanoplatform for photodynamic therapy and chemotherapy of triple-negative breast cancer. *Chin Chem Lett.* 2023;34(12):1–10. doi:10.1016/j.cclet.2023.108332

15. Taha S, Mohamed WR, Elhemely MA, El-Gendy AO, Mohamed T. Tunable femtosecond laser suppresses the proliferation of breast cancer in vitro. *J Photochem Photobiol B: Biol.* 2023;240(1):1–8. doi:10.1016/j.jphotobiol.2023.112665

16. Sleire L, Førde HE, Netland IA, Leiss L, Skeie BS, Enger PØ. Drug repurposing in cancer. *Pharmacol Res.* 2017;124(1):74–91. doi:10.1016/j.phrs.2017.07.013

17. Crofts TS, Sontha P, King AO, et al. Discovery and characterization of a nitroreductase capable of conferring bacterial resistance to chloramphenicol. *Cell Chem Biol.* 2019;26(4):559–570. doi:10.1016/j.chembiol.2019.01.007

18. Andrade JK, Souza MI, Gomes Filho MA, et al. N-pentyl-nitrofurantoin induces apoptosis in HL-60 leukemia cell line by upregulating BAX and downregulating BCL-xL gene expression. *Pharmacol Rep.* 2016;68(5):1046–1053. doi:10.1016/j.pharep.2016.06.004

19. Race PR, Lovering AL, Green RM, et al. Structural and mechanistic studies of Escherichia coli nitroreductase with the antibiotic nitrofurazone: reversed binding orientations in different redox states of the enzyme. *J Biol Chem.* 2005;280(14):13256–13264. doi:10.1074/jbc.M409652200

20. Wang Y, Gray JP, Mishin V, Heck DE, Laskin DL, Laskin JD. Role of cytochrome P450 reductase in nitrofurantoin-induced redox cycling and cytotoxicity. *Free Radic Biol Med.* 2008;44(6):1169–1179. doi:10.1016/j.freeradbiomed.2007.12.013

21. Al-Masoudi NA, Al-Soud YA, Kalogerakis A, Pannecouque C, De Clercq E. Nitroimidazoles, part 2: synthesis, antiviral and antitumor activity of new 4- nitroimidazoles. *Chem Biodivers.* 2006;3(5):515–526. doi:10.1002/cbdv.200690055

22. Chen Z, Han F, Du Y, Shi H, Zhou W. Hypoxic microenvironment in cancer: molecular mechanisms and therapeutic interventions. *Signal Transduct Target Ther.* 2023;8(1):70–82. doi:10.1038/s41392-023-01332-8

23. Manin AN, Voronin AP, Boycov DE, Drozd KV, Churakov AV, Perlovich GL. A combination of virtual and experimental screening tools for the prediction of nitrofurantoin multicomponent crystals with pyridine derivatives. *Crystals.* 2023;13(7):1022. doi:10.3390/cryst13071022

24. Dadwal A, Baldi A, Kumar Narang R. Nanoparticles as carriers for drug delivery in cancer. *Artif Cells Nanomed Biotechnol.* 2018;46(1):295–305. doi:10.1080/21691401.2018.1457039

25. Yao Y, Zhou Y, Liu L, et al. Nanoparticle-based drug delivery in cancer therapy and its role in overcoming drug resistance. *Front Mol Biosci.* 2020;7(1):1–14. doi:10.3389/fmolb.2020.00193

26. Khan R, Arshad A, Hassan IU, et al. Advances in nanomaterial-based immunosensors for prostate cancer screening. *Biomed Pharmacother.* 2022;155(1):1–12. doi:10.1016/j.biopha.2022.113649

27. El-Laithy H, Badawi A, Abdelmalak NS, El-Sayyad N. Cubosomes as oral drug delivery systems: a promising approach for enhancing the release of clopidogrel bisulphate in the intestine. *Chem Pharm Bull.* 2018;66(12):1165–1173. doi:10.1248/cpb.c18-00615

28. Varghese R, Salvi S, Sood P, Kulkarni B, Kumar D. Cubosomes in cancer drug delivery: a review. *Colloids Interface Sci Commun.* 2022;46(1):1–11. doi:10.1016/j.colcom.2021.100561

29. Garg G, Saraf S, Saraf S. Cubosomes: an overview. *Biol Pharm Bull.* 2007;30(1):350–353. doi:10.1248/bpb.30.350

30. Shetty S, Shetty S. Cubosome-based cosmeceuticals: a breakthrough in skincare. *Drug Discov Today.* 2023;28(7):103623. doi:10.1016/j.drudis.2023.103623

31. Zhang L, Li J, Tian D, Sun L, Wang X, Tian M. Theranostic combinatorial drug-loaded coated cubosomes for enhanced tar geting and efficacy against cancer cells. *Cell Death Dis.* 2020;11(1):1.

32. Murgia S, Falchi AM, Mano M, et al. Nanoparticles from lipid-based liquid crystals: emulsifier influence on morphology and cytotoxicity. *J Phys Chem B.* 2010;114(10):3518–3525. doi:10.1021/jp9098655

33. Yaghmur A, Glatter O, Characterization and potential applications of nanostructured aqueous dispersions. *Adv Colloid Interface Sci.* 2009;147-148(1):333–342. doi:10.1016/j.cis.2008.07.007

34. Janakiraman K, Krishnaswami V, Sethuraman V, Rajendran V, Kandasamy R. Development of methotrexate-loaded cubosomes with improved skin permeation for the topical treatment of rheumatoid arthritis. *Appl Nanosci.* 2019;9(3):1781–1796. doi:10.1007/s13204-019-00976-9

35. Madheswaran T, Kandasamy M, Bose R, Karuppagounder V. Current potential and challenges in the advances of liquid crystalline nanoparticles as drug delivery systems. *Drug Discov Today.* 2019;24(7):1405–1412. doi:10.1016/j.drudis.2019.05.004

36. Lars L, Sandra W, Ajay Vikram S, Peter L, Andreas L. Nanoparticle induced barrier function assessment at liquid–liquid and air–liquid interface in novel human lung epithelia cell lines. *Toxicol Res.* 2019;8(1):1016–1027. doi:10.1039/c9tx00179d

37. Sivadasan D, Sultan MH, Alqahtani SS, Javed S. Cubosomes in drug delivery—a comprehensive review on its structural componen ts, preparation techniques and therapeutic applications. *Biomedicines.* 2023;11(4):1114–1139. doi:10.3390/biomedicines11041114

38. Siekmann B, Bunjes H, Koch MH, Westesen K. Preparation and structural investigations of colloidal dispersions prepared from cubic mono-glyceride water phases. *Int J Pharm.* 2002;244(1–2):33–43. doi:10.1016/S0378-5173(02)00298-3

39. Meli V, Caltagirone C, Falchi AM, et al. Docetaxel-loaded fluorescent liquid-crystalline nanoparticles for cancer theranostics. *Langmuir ACS J Surf Colloids.* 2015;31(35):9566–9575. doi:10.1021/acs.langmuir.5b02101

40. Salema EM, Dawabaa HM, Gadc S, Hassanc TH. Cubosomes as an Oral Drug Delivery System. *Rec Pharm Biomed Sci.* 2023;7(3):81–90.

41. Umar HA, Wahab H, Gazzali AM, Tahir H, Ahmed W. Cubosomes: design, development, and tumor-targeted drug delivery applications. *Polymers (Basel)*. 2022;14(15):3118–3136. doi:10.3390/polym14153118

42. El-Hashemy HA, Salama A, Rashad A. Experimental design, formulation, and in-vivo evaluation of novel anticoagulant Rivaroxaban loaded cubosomes in rats model. *J Liposome Res*. 2022;1(1):1–8.

43. Zewail M, Gaafar PME, Ali MM, Abbasa H. Lipidic cubic-phase leflunomide nanoparticles (cubosomes) as a potential tool for breast cancer management. *Drug Deliv*. 2022;29(1):1663–1674. doi:10.1080/10717544.2022.2079770

44. Nasr M, Younes H, Abdel-Rashid RS. Formulation and evaluation of cubosomes containing colchicine for transdermal delivery. *Drug Deliv Transl Res*. 2020;10(1):1302–1313. doi:10.1007/s13346-020-00785-6

45. Cair MR, Pienaar EW, Lotter AP. Polymorphism and pseudopolymorphism of the antibacterial nitrofurantoin. *Mol Cryst Liq Cryst*. 1996;279 (1):241–264. doi:10.1080/10587259608042194

46. Marques C, Maurizi L, Borchard G, Jordan O. Characterization challenges of self-assembled polymer-SPIONs nanoparticles: benefits of orthogonal methods. *Int J Mol Sci*. 2022;23(1):1–17. doi:10.3390/ijms232416124

47. Hashem F, Nasr M, Youssif M. Formulation and characterization of cubosomes containing REB for improvement of oral absorption of the drug in human volunteers. *J Adv Pharm Res*. 2018;2(2):95–103. doi:10.21608/aprh.2018.5828

48. Elsayad M, Mowafy HA, Zaky AA, Samy AA. Chitosan caged liposomes for improving oral bioavailability of rivaroxaban: in vitro and in vivo evaluation. *Pharm Dev Technol*. 2021;26(3):316–327. doi:10.1080/10837450.2020.1870237

49. Chettupalli AK, Ananthula M, Amarachinta PR, Bakshi V, Yata VK. Design, formulation, in-vitro and ex-vivo evaluation of atazanavir loaded cubosomal gel. *Biointerface Res Appl Chem*. 2021;11(4):12037–12054.

50. Kamel AA, Fadel M, Louis D. Curcumin-loaded nanostructured lipid carriers prepared using Peceol™ and olive oil in photodynamic therapy: development and application in breast cancer cell line. *Int J Nanomed*. 2019;14(1):5073–5085. doi:10.2147/IJN.S210484

51. Shah M, Pathak K. Development and statistical optimization of solid lipid nanoparticles of simvastatin by using 23 full-factorial design. *AAPS Pharm Sci Tech*. 2010;11(2):489–496. doi:10.1208/s12249-010-9414-z

52. Flak DK, Adamski V, Nowaczyk G, et al. AT101-loaded cubosomes as an alternative for improved glioblastoma therapy. *Int J Nanomed*. 2020;15 (1):7415–7431. doi:10.2147/IJN.S265061

53. Segalina A, Pavan B, Ferretti V, et al. Cocrystals of nitrofurantoin: how coformers can modify its solubility and permeability across intestinal cell monolayers. *Cryst Growth Des*. 2022;22(5):3090–3106. doi:10.1021/acs.cgd.2c00007

54. S HAN, Shen J, Y GAN, et al. Novel vehicle based on cubosomes for ophthalmic delivery of flurbiprofen with low irritancy and high Bioavailability. *Acta Pharmacol Sin*. 2010;31(1):990–998. doi:10.1038/aps.2010.98

55. Nasr M, Ghorab MK, A A. In vitro and in vivo evaluation of cubosomes containing 5-fluorouracil for liver targeting. *Acta Pharm Sin B*. 2015;5 (1):79–88. doi:10.1016/j.apsb.2014.12.001

56. Hakim E, El-Mahrouk GM, Abdelbary G, Teaima MH. Freeze-dried clopidogrel loaded lyotropic liquid crystal: box-behnken optimization, in-vitro and in-vivo evaluation. *Curr Drug Deliv*. 2020;17(3):207–217. doi:10.2174/1567201817666200122161433

57. Abdel-Bar HM, Sanad RA. Endocytic pathways of optimized resveratrol cubosomes capturing into human hepatoma cells. *Biomed Pharmacother*. 2017;93(1):561–569. doi:10.1016/j.biopha.2017.06.093

58. Zaki RM, Abou El Ela AE, Almurshedi AS, Aldosari BN, Aldossari AA, Ibrahim MA. Fabrication and assessment of orodispersible tablets loaded with cubosomes for the improved anticancer activity of simvastatin against the MDA-MB-231 breast cancer cell line. *Polymers*. 2023;15 (7):1774–1788. doi:10.3390/polym15071774

59. Adepu S, Ramakrishna S. Controlled drug delivery systems: current status and future directions. *Molecules*. 2021;26(19):1–45. doi:10.3390/molecules26195905

60. Lu S, Wei L, He W, et al. Recent advances in the enzyme-activatable organic fluorescent probes for tumor imaging and therapy. *ChemistryOpen*. 2022;11(10):1–11. doi:10.1002/open.202200137

61. Almoshari Y, Alam MI, Bakkari MA, et al. Formulation, characterization, and evaluation of doxorubicin-loaded cubosome as a cytotoxic potentiator against HCT-116 colorectal cancer cells. *Indian J Pharm Educ Res*. 2022;56(3):723–731. doi:10.5530/ijper.56.3.121